Analysis of sucrose accumulation in the sugar cane culm on the basis of *in vitro* kinetic data

Johann M. ROHWER*[1] and Frederik C. BOTHA†

*Department of Biochemistry, University of Stellenbosch, Private Bag X1, 7602 Matieland, South Africa, and †Institute for Plant Biotechnology, University of Stellenbosch, Private Bag X1, 7602 Matieland, South Africa

Sucrose accumulation in developing sugar cane (*Saccharum officinarum*) is accompanied by a continuous synthesis and cleavage of sucrose in the storage tissues. Despite numerous studies, the factors affecting sucrose accumulation are still poorly understood, and no consistent pattern has emerged which pinpoints certain enzyme activities as important controlling steps. Here, we develop an approach based on pathway analysis and kinetic modelling to assess the biochemical control of sucrose accumulation and futile cycling in sugar cane. By using the concept of elementary flux modes, all possible routes of futile cycling of sucrose were enumerated in the metabolic system. The available kinetic data for the pathway enzymes were then collected and assembled in a kinetic model of sucrose accumulation in sugar cane culm tissue. Although no data were fitted, the model agreed well with independent experimental results: in no case was the difference between calculated and measured fluxes and concentrations greater than 2-fold. The model thus validated was then used to assess different enhancement strategies for increasing sucrose accumulation. First, the control coefficient of each enzyme in the system on futile cycling of sucrose was calculated. Secondly, the activities of those enzymes with the numerically largest control coefficients were varied over a 5-fold range to determine the effect on the degree of futile cycling, the conversion efficiency from hexoses into sucrose, and the net sucrose accumulation rate. In view of the modelling results, overexpression of the fructose or glucose transporter or the vacuolar sucrose import protein, as well as reduction of cytosolic neutral invertase levels, appear to be the most promising targets for genetic manipulation. This offers a more directed improvement strategy than cumbersome gene-by-gene manipulation. The kinetic model can be viewed and interrogated on the World Wide Web at http://jjj.biochem.sun.ac.za.

Key words: control analysis, futile cycling, kinetic modelling, metabolic engineering, pathway analysis.

INTRODUCTION

Dry matter accumulation and sucrose content increase sharply within the top internodes in developing sugar cane (*Saccharum officinarum*) [1–3]. The increase in sucrose content during internode maturation coincides with a repartitioning of carbon from insoluble matter and respiration towards sucrose storage [3]. Sucrose accumulation is not merely a function of time, since the rate of accumulation significantly increases between young and more mature internodes [3,4]. Although it is well known that significant differences in sucrose content are evident between different sugar cane varieties, the biochemical basis for this is still poorly understood.

Traditionally, identification of key regulatory reactions in metabolism was based on the assumptions that these would be largely irreversible, that the enzymes would be regulated and reciprocal changes in flux and substrate concentrations would be evident. However, it is now obvious that this approach is very limited because it does not consider the correlation between enzyme activity and actual flux within the system [5]. The severe limitation by this traditional approach is evident from the numerous examples of unexpected effects where specific genes were genetically manipulated in plants.

Current knowledge about sucrose accumulation in sugar cane is largely based on the traditional approach. Sucrose is accumulated against a gradient, the energy for which is provided by respiration. It is evident that sucrose accumulation is accompanied by a continuous cleavage and synthesis of sucrose during accumulation of sucrose in storage tissue [3,6,7] and cell-suspension cultures [8]. Numerous studies on enzyme activities that can potentially be important in these processes have been carried out, but no consistent pattern has emerged from these studies. In some varieties, soluble acid invertase activity decreases sharply during maturation [9–11], in others this is not evident [12]. Sucrose phosphate synthase activity is sometimes induced [4] or remains constant [11]. Sucrose synthase can either increase [13] or decrease [4]. Currently, a model that predicts that sucrose accumulation is dependent on a system in which sucrose phosphate synthase activity exceeds that of acid invertase is favoured [11]. However, the complexity of the system and all the potential permutations makes it virtually impossible to identify the reactions that could be good targets for genetic manipulation in an attempt to increase the sucrose load.

Instead of a cumbersome gene-by-gene manipulation strategy, we have followed a strategy based on pathway analysis (e.g. [14,15]) and kinetic modelling (e.g. [16,17]) to study sucrose accumulation in sugar cane. In a first approach using elementary modes [18], all possible routes of futile cycling (synthesis and breakdown) of sucrose were determined. Subsequently, we developed a detailed kinetic model to investigate factors determining sucrose accumulation and futile cycling. Such a model could be an invaluable tool to predict the most likely control

Abbreviation used: hexokinase(Glc), hexokinase (glucose phosphorylating).

[1] To whom correspondence should be addressed (e-mail jr@maties.sun.ac.za).

points of processes that lead to sucrose accumulation. Substantial information is already available [3] to validate the performance of such a model. Using the model, we are able to assess different manipulation strategies on their potential to enhance sucrose accumulation and select the most promising ones.

METHODS

Metabolic system delineation

The present study deals with sucrose accumulation by the sugar cane culm. The photosynthetic product sucrose is transported in the phloem from the leaves to the culm, where it is off-loaded, hydrolysed, and a significant portion taken up as glucose and fructose [19]. In the cytoplasm of the culm cells, sucrose is synthesized in a number of reactions (summarized in Figure 1), and the sucrose is transported into the vacuole where it is accumulated. To restrict the model to those reactions directly involved in sucrose synthesis and accumulation, we lumped all reactions of the lower part of glycolysis from fructose 6-phosphate into a single reaction block.

Elementary mode analysis

Elementary flux modes were calculated with the computer program METATOOL [20].

Numerical methods

Steady-state calculations of the kinetic models were performed on an IBM-compatible personal computer with the metabolic

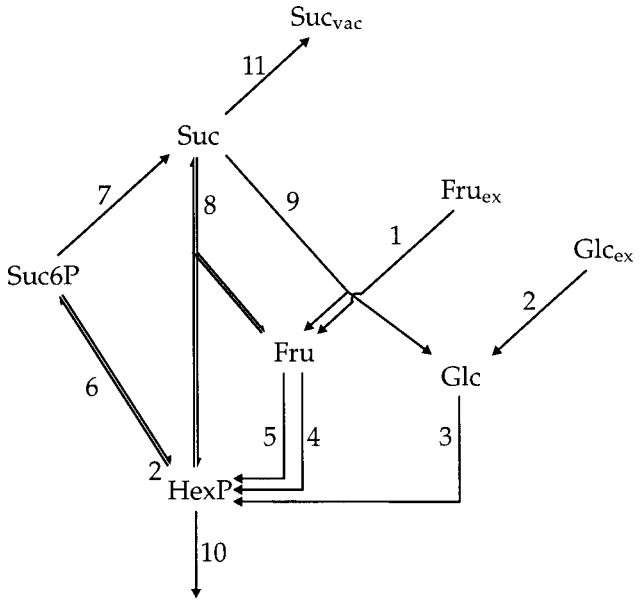

Figure 1 Sucrose accumulation in sugar cane culm tissue

Reactions: 1, fructose (Fru) uptake; 2, glucose (Glc) uptake; 3, hexokinase(Glc); 4, hexokinase (fructose phosphorylating); 5, fructokinase; 6, sucrose phosphate synthase; 7, sucrose phosphate phosphatase; 8, sucrose synthase; 9, invertase; 10, glycolysis; 11, vacuolar sucrose import. Reaction 6 is defined forward in the direction of sucrose 6-phosphate (Suc6P) synthesis, and has a stoichiometry of 2 for HexP (fructose 6-phosphate and UDP-glucose). Reaction 8 is defined forward in the direction of sucrose (Suc) synthesis. The hexose phosphate pool was considered as an equilibrium block comprising UDP-glucose, glucose 1-phosphate, glucose 6-phosphate and fructose 6-phosphate. HexP, hexose phosphates; subscript 'ex', extracellular; subscript 'vac', vacuolar.

Table 1 Kinetic parameters of the enzyme-catalysed reactions

All maximal rates are in mM/min and all K_m and K_i values are in mM.

Reaction/parameter	Value	Reference	Comment
Reaction 1: fructose uptake			
V_{max1}	0.286	[32]	
$K_{m\ Fruex}$	0.2	[19,33]	
$K_{i\ Fru}$	1		Estimate
Reaction 2: glucose uptake			
V_{max2}	0.286	[32]	
$K_{m\ Glcex}$	0.2	[19,33]	
$K_{i\ Glc}$	1		Estimate
Hexokinase. Reaction 3: glucose phosphorylating, reaction 4: fructose phosphorylating			
V_{max3}	0.197	[34,35]	
V_{max4}	0.197	[34,35]	
$K_{m\ Glc}$	0.07	[36]	Range 0.03–0.13
$K_{m\ Fru}$	10	[37]	Range 8.7–22
$K_{m\ ATP}$	0.25	[36]	Range 0.1–0.56
$K_{i\ Glc6P}$	0.1		Estimate
$K_{i\ Fru6P}$	10		Estimate
Reaction 5: fructokinase			
V_{max5}	0.164	[34,35]	
$K_{m\ Fru}$	0.1	[36,38]	Range 0.04–0.22
$K_{m\ ATP}$	0.085	[38,39]	Range 0.046–0.67
$K_{i\ ADP}$	2	[38,39]	Range 1–5
$K_{i\ Fru}$	12	[36,38,39]	Range 1–21
Reaction 6: sucrose phosphate synthase			
K_{eq6}	10	[30]	
V_{f6}	0.379	[34]	
V_{r6}	0.2		Estimate
$K_{m\ Fru6P}$	0.6	[40,41]	Range 0.3-2
$K_{m\ UDPGlc}$	1.8	[40,41]	Range 1.2-3
$K_{m\ UDP}$	0.3		Estimate, similar to measured UDP concentration
$K_{m\ Suc6P}$	0.1		Estimate, same as K_m of sucrose phosphatase
$K_{i\ Pi}$	3	[40]	Range 0.2–5
$K_{i\ Fru6P}$	0.4		Estimate
$K_{i\ UDPGlc}$	1.4		Estimate
$K_{i\ Suc6P}$	0.07		Estimate
Reaction 7: sucrose phosphatase			
V_{max7}	0.5	[41]	
$K_{m\ Suc6P}$	0.1	[41]	Range 0.045–0.15
Reaction 8: sucrose synthase			
K_{eq8}	5	[30]	
V_{f8}	0.677	[34]	
V_{r8}	0.3	[34]	
$K_{m\ Suc}$	50	[31,41]	Range 10–400
$K_{m\ UDP}$	0.3	[31,41]	Range 0.1–1.7
$K_{m\ UDPGlc}$	0.3	[31,41]	Range 0.1–5
$K_{m\ Fru}$	4	[31,42]	Range 1.6–8
$K_{i\ Fru}$	4		Assumed equal to $K_{m\ Fru}$
$K_{i\ UDP}$	0.3		Assumed equal to $K_{m\ UDP}$
$K_{i\ Suc}$	40	[31]	
Reaction 9: neutral invertase			
V_{max9}	0.372	[43]	
$K_{m\ Suc}$	10	[43]	
$K_{i\ Fru}$	15	[29,43]	
$K_{i\ Glc}$	15	[29,43]	
Reaction 10: lower glycolysis			
V_{max10}	0.1	[32,35]	Based on respiratory flux measured with labelled hexoses
$K_{m\ Fru6P}$	0.2	[35]	Average substrate affinity of phosphofructokinase and pyrophosphate-dependent phosphofructokinase
Reaction 11: sucrose accumulation into vacuole			
V_{max11}	1		Estimate
$K_{m\ Suc}$	100		Estimate

Table 1 (contd.)

Reaction/parameter	Value	Reference	Comment
UDP-glucose pyrophosphorylase			
K_{eq}	0.312	[30]	Direction of glucose 1-phosphate formation
Phosphoglucomutase			
K_{eq}	17.6	[30]	Direction of glucose 6-phosphate formation
Phosphoglucoisomerase			
K_{eq}	0.509	[30]	Direction of fructose 6-phosphate formation

Table 2 Fixed metabolite concentrations of the kinetic model

Fru_{ex}, extracellular fructose; Glc_{ex}, extracellular glucose.

Metabolite	Concentration (mM)	Reference	Comment
Fru_{ex}	5	[44]	Substrate levels during labelling experiments
Glc_{ex}	5	[44]	Substrate levels during labelling experiments
ATP	1	[31]	Range 0.5–2 mM
ADP	0.2	[31]	ATP/ADP range 3–7
UDP	0.2		Assumed equal to ADP
P_i	5.1	[35]	

modelling program WinScamp [21]. The calculations were checked with Gepasi [22].

Kinetics of enzyme-catalysed reactions

The differential equations describing the time-dependence of the variable metabolite concentrations, as well as the rate equations used for simulating the enzyme-catalysed reactions, are summarized in the Appendix.

Model parameters

The kinetic parameters used for the model are summarized in Table 1. Values for kinetic constants were taken from the literature where available, and estimated otherwise as indicated in the Table. Maximal enzyme activities were taken as determined for culm tissue from internode 5, reflecting medium-mature tissue. For conversion, 1 g (fresh weight) of tissue was assumed to correspond to an intracellular volume of 700 μl [3], with 10 % cytoplasmic and 90 % vacuolar volume [23].

In order for the model to be able to calculate a steady state, the concentrations of the terminal boundary metabolites (source and sink) need to be fixed. We entered these as measured in internode 5 tissue. In addition, the cofactors ATP, ADP and UDP, as well as phosphate, were not modelled as explicit system variables, but their concentrations were entered as constants. The fixed metabolite concentrations are summarized in Table 2.

Control analysis

Metabolic control analysis is a quantitative framework originally developed by Kacser and Burns [24] and Heinrich and Rapoport [25] to quantify the control of the steady-state behaviour of metabolic systems. The extent to which any catalytic step (e.g. an enzyme-catalysed reaction) controls a steady-state metabolic variable (flux or concentration) is quantified by a control coefficient, which, for a step i of the system, is defined [26] as:

$$C_i^y = [(\partial \ln|y|/\partial p_i)_{p_k}]/[(\partial \ln|v_i|/\partial p_i)_{s_j, p_k}] \quad (1)$$

where y is the steady-state variable, and p_i is any parameter that affects step i specifically (e.g. the concentration of enzyme i or a specific inhibitor for step i). Subscript p_k indicates that the other parameters p_k remain constant and that the entire system relaxes to a new steady state after a change in p_i; subscript s_j,p_k indicates that the change in the rate v_i of the independent step i is considered locally at constant reactant and product concentrations [27].

In the present paper we use control analysis to identify those steps that most significantly affect futile cycling of sucrose.

RESULTS

Isotope-labelling studies have revealed significant futile cycling in sucrose-accumulating sugar cane tissue, in that approx. 30 % of the sucrose synthesized is re-hydrolysed to glucose and fructose [3]. Futile cycling is an energetically expensive process, because nucleoside triphosphates are required in a number of steps (ATP in the hexokinase and fructokinase reactions, and UTP for the synthesis of UDP-glucose, which is a substrate of the sucrose phosphate synthase and sucrose synthase reactions). A significant percentage of futile cycling of sucrose might, therefore, lead to reduced sucrose accumulation. In contrast, if futile cycling of sucrose could be reduced, this might lead to improved sucrose accumulation and agricultural yields.

The metabolic system of sucrose synthesis (Figure 1) is highly branched. It is difficult to predict by inspection the flux distribution through this system for different conditions, let alone the factors that determine this distribution. A useful tool in our analysis was the concept of an elementary flux mode, defined as a non-decomposable set of reactions that can carry a steady-state flux in a metabolic system [18]. Any steady-state flux distribution can be written as a linear combination of different elementary flux modes, and moreover, the full set of elementary modes is uniquely defined for every metabolic system. A complete elementary mode analysis will: (i) show up all the futile cycles in the system; (ii) determine all possible routes from a given pathway substrate to a product; and (iii) predict which metabolic

Table 3 Elementary flux modes in sucrose biosynthesis

Elementary modes were calculated by the program METATOOL [20] with the stoichiometry of Figure 1 as input. All 14 elementary modes are irreversible and proceed only in the direction indicated. Fru_{ex}, extracellular fructose; Glc_{ex}, extracellular glucose; Suc_{vac}, vacuolar sucrose.

Mode number	Sequence of steps	Net reaction
1	R3 → R8 → R9	–
2	R4 → R6 → R7 → (−R8)	–
3	R5 → R6 → R7 → (−R8)	–
4	R3 → R4 → R6 → R7 → R9	–
5	R3 → R5 → R6 → R7 → R9	–
6	R1 → R4 → R10	Fru_{ex} → glycolysis
7	R1 → R5 → R10	Fru_{ex} → glycolysis
8	R2 → R3 → R10	Glc_{ex} → glycolysis
9	(2 × R1) → (2 × R4) → R6 → R7 → R11	2 Fru_{ex} → Suc_{vac}
10	(2 × R1) → (2 × R5) → R6 → R7 → R11	2 Fru_{ex} → Suc_{vac}
11	(2 × R2) → (2 × R3) → R6 → R7 → R11	2 Glc_{ex} → Suc_{vac}
12	(2 × R1) → R4 → R8 → R11	2 Fru_{ex} → Suc_{vac}
13	(2 × R1) → R5 → R8 → R11	2 Fru_{ex} → Suc_{vac}
14	R1 → R2 → R3 → R8 → R11	Fru_{ex} + Glc_{ex} → Suc_{vac}

Table 4 Steady-state properties of the kinetic model

(a)

Step	Enzyme	Flux (mM/min)
R1	Fructose uptake	0.107
R2	Glucose uptake	0.127
R3	Hexokinase(Glc)	0.155
R4	Hexokinase(Fru)	0.0015
R5	Fructokinase	0.034
R6	Sucrose phosphate synthase	0.023
R7	Sucrose phosphatase	0.023
R8	Sucrose synthase	0.099
R9	Invertase (neutral)	0.027
R10	Lower glycolysis	0.046
R11	Vacuolar sucrose accumulation	0.094

(b)

Metabolite	Concentration (mM)
Fructose	40.6
Glucose	30.1
Sucrose	10.4
Sucrose 6-phosphate	0.005
UDP-glucose	2.46
Glucose 1-phosphate	0.019
Glucose 6-phosphate	0.337
Fructose 6-phosphate	0.172

Table 5 Kinetic model validation: comparison of calculated and experimentally determined fluxes and metabolite concentrations

The calculated fluxes and concentrations are from Table 4. Experimental values are taken from the references indicated. All values refer to cytosolic metabolite concentrations.

(a)

	Flux (mM/min)	
Step	Model	Experiment
Glucose uptake	0.127	0.195 [32]
Hexokinase(Glc)	0.155	0.197 [32]
Glycolysis	0.046	0.041 [32]
Net sucrose accumulation	0.094	0.127 [32]

(b)

	Concentration (mM)	
Metabolite	Model	Experiment
Glucose	30	29 [3]
Fructose	41	30 [3]
UDP-glucose	2.46	2.67 [45]
Glucose 6-phosphate	0.34	0.21 [3]
Fructose 6-phosphate	0.17	0.12 [3]

routes produce the product with the highest molar yield. It is therefore possible to distinguish between higher-yielding and lower-yielding pathways, should these exist.

We used the computer program METATOOL [20] to calculate all elementary flux modes for the sucrose system (Table 3). The first remarkable result is that five of the 14 modes (1–5) are futile cycles, not leading to any product. In one of these (mode 1) the sucrose synthase reaction proceeds in the direction of sucrose synthesis, whereas in two others (modes 2 and 3) the enzyme works in the other direction. In all futile cycle modes sucrose is synthesized and broken down again [either by invertase (modes 1, 4 and 5) or by sucrose synthase (modes 2 and 3)]. Strictly speaking, the net reaction of the futile cycles is not zero, but rather hydrolysis of ATP into ADP (Figure 1, reactions 3–5), or UTP to PPi (reactions 6 and 8), or both. This is not apparent in Table 3 since we treated those cofactors as constants and did not include them explicitly in the stoichiometric analysis; however, it emphasizes the fact that futile cycling of sucrose is an energetically expensive process.

The remaining elementary modes either break down hexoses in glycolysis (modes 6–8) or synthesize sucrose from hexoses (modes 9–14). As expected, two hexose moieties are always required for sucrose synthesis; these can both originate from fructose (modes 9, 10, 12 and 13), or both from glucose (mode 11), or one from each of them (mode 14).

While an elementary mode analysis will point out futile cycles and optimal conversion pathways for product synthesis, it cannot ascertain which factors will influence the flux distribution in a metabolic network and cause a shift from one mode to another, since it considers only stoichiometric information. Yet metabolic behaviour depends not only on stoichiometry, but also on thermodynamics and kinetics. To understand the dynamics of sucrose accumulation more fully, we combined the known kinetic and thermodynamic information of the enzymes involved into a detailed kinetic model (see the Appendix). The values of the steady-state properties as calculated by the model are summarized in Table 4 for the parameter set of Table 1. Importantly, in agreement with experimental results [3], the model predicts significant futile cycling of sucrose, in that 22% of the sucrose synthesized is broken down again by invertase, $J_9/(J_9+J_{11}) = 0.22$. We have subsequently coded the kinetic model in Java and Mathematica, so that it can be viewed and interrogated live on the World Wide Web from our research group's website at http://jjj.biochem.sun.ac.za.

The kinetic model described here assembles the known kinetic and thermodynamic data for all the different enzymes into a whole. This does not mean *a priori* that any results calculated by the model will be an accurate reflection of experimentally observed reality. The model first needs to be validated and its performance assessed by comparing it with independent experimental observations. Table 5 compares the fluxes and steady-state concentrations of the variable metabolites calculated by the model with those determined experimentally in sugar cane culm tissue. In general, the values agreed well (in all cases, model and experiment differed by less than a factor of two). It should be emphasized that no model parameters were fitted; the kinetic data were taken from the literature and entered directly into the model, after which the calculated fluxes and concentrations were compared with independent experimental data.

Having developed a kinetic model that describes the metabolism of sucrose accumulation in sugar cane culm, we next investigated which of the reactions would have the greatest effect on futile cycling of sucrose, i.e. the partitioning of flux between sucrose accumulation into the vacuole (Figure 1, reaction 11) and sucrose hydrolysis by invertase (reaction 9). We assessed these effects by calculating (using the model) for each step i its futile cycling control coefficient $C_i^{J_9/J_{11}}$ (see eqn 1 for general definition). Note that $C_i^{J_9/J_{11}} = C_i^{J_9} - C_i^{J_{11}}$. The values for the futile cycling control coefficients calculated by the model are summarized in Figure 2. The steps for fructose uptake, glucose uptake, hexokinase (glucose phosphorylating) [hexokinase(Glc)], invertase and vacuolar sucrose accumulation had the greatest

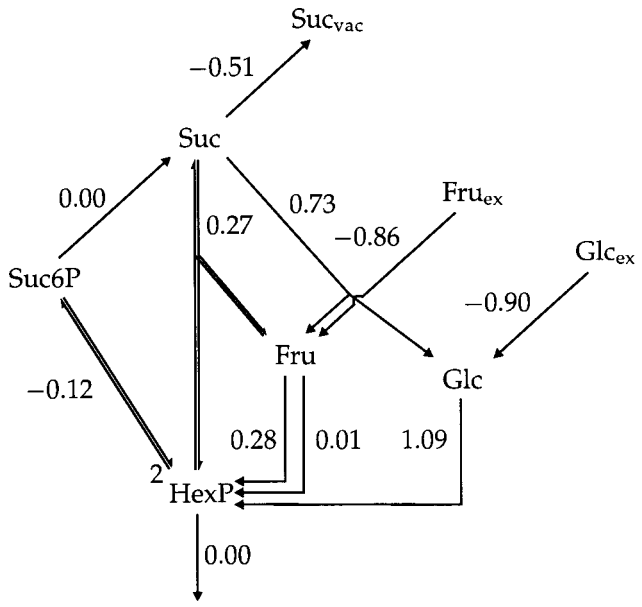

Figure 2 Futile cycling control coefficients

For each step, the value of the futile cycling control coefficient $C_i^{J_9/J_{11}}$ was calculated as described in the text. The value, as calculated by the model, is indicated alongside the arrow for the respective reaction. The control coefficient describes to what extent that step controls the flux partitioning between neutral invertase (reaction 9) and sucrose accumulation (reaction 11). Abbreviations defined in Figure 1 legend.

effect on the futile cycling ratio. Fructose and glucose uptake, as well as vacuolar sucrose accumulation, had negative control coefficients, implying a decreased J_9/J_{11} (and therefore decreased futile cycling of sucrose) upon an increase in the activity of those particular steps. Conversely, hexokinase(Glc) and invertase had positive control coefficients, implying increased futile cycling upon an increase in those steps' activity.

So far we have identified the reactions with the greatest control on futile cycling of sucrose. It is an important question what would happen to the behaviour of the system should one or more of these reactions now be manipulated. Because control coefficients are defined using infinitesimal changes around an asymptotically stable steady state, their values for one specific steady state are not generally extrapolatable to more distant steady states. Hence, when increasing an enzyme activity by, say, 3-fold, it is generally impossible to calculate the new steady state only from the control coefficients and the reference steady state. Here, kinetic modelling is an extremely powerful tool, because it enables one to explore 'what if?' scenarios by changing one or more model parameters and calculating the resultant behaviour. We applied this approach to those steps in our system targeted by the control analysis (i.e. the steps predicted to have the greatest effect on futile cycling of sucrose). We increased the activities of the steps with negative $C_i^{J_9/J_{11}}$ from their reference values up to 5-fold, calculating the effects on the flux towards vacuolar sucrose accumulation (J_{11}), the percentage of futile cycling [$J_9/(J_7+J_8)$], and the net conversion efficiency of hexoses into sucrose [$2J_{11}/(J_1+J_2)$]. The activities of the steps with positive $C_i^{J_9/J_{11}}$ were decreased analogously (Figure 3).

As predicted by the control coefficients, the manipulations in enzyme activity led to a decrease in futile cycling in all cases (Figure 3). The increase in the activity of the fructose uptake step (Figure 3a) and the decrease in the activity of hexokinase-(Glc) (Figure 3c) led to a concomitant increase in the conversion efficiency, i.e. the percentage of hexoses converted into sucrose; this percentage remained more or less constant for the other cases. Finally, in all cases except for the hexokinase(Glc) manipulation, the enzyme activity changes led to an increase in the flux of vacuolar sucrose accumulation, J_{11}, with the greatest

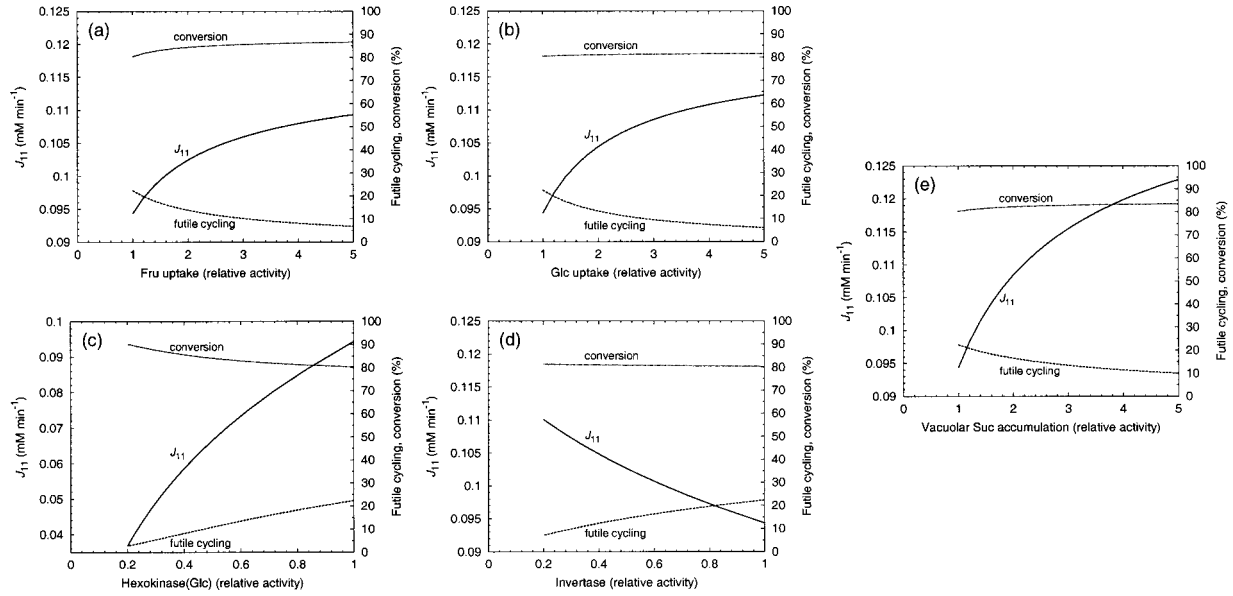

Figure 3 Effect of manipulating enzyme activities on sucrose accumulation and futile cycling

For each step shown, the V_{max} was increased or decreased up to 5-fold from its reference level (Table 1) as indicated. The flux towards vacuolar sucrose accumulation (J_{11}), the percentage of futile cycling [$J_9/(J_7+J_8)\times 100$], and the net conversion of hexoses into sucrose [$2\ J_{11}/(J_1+J_2)\times 100$] were calculated with the model as a function of these enzyme manipulations. (**a**) Fructose uptake-, (**b**) glucose uptake-, (**c**) hexokinase(Glc)-, (**d**) invertase-, and (**e**) vacuolar sucrose accumulation-profiles.

increase observed for the manipulation of vacuolar sucrose import activity (Figure 3). While the decrease of hexokinase(Glc) to 20% of its reference level reduced futile cycling to less than 5%, the flux of sucrose accumulation (J_{11}) decreased to approximately one third of its original value at the same time (Figure 3c).

DISCUSSION

This paper describes a pathway analysis, kinetic model and control analysis of sucrose metabolism in medium-mature sugar cane culm. We set out by delineating the problem that the factors controlling sucrose accumulation in sugar cane are at present not fully understood. Because the pathways around sucrose are highly branched (Figure 1), we used a structural analysis to find all the elementary modes, i.e. all possible elementary steady-state flux distributions (Table 3). This analysis, in addition, detected all possible futile cycles in the metabolic system, some of which are energetically wasteful.

Because futile cycling of sucrose has been observed experimentally [3] and is predicted to affect sucrose accumulation, we combined all the available kinetic data for the pathway enzymes into a detailed kinetic model. The steady-state intermediate concentrations calculated by the model agreed well with independent direct determinations, although no kinetic parameters were fitted. We did not fit the parameters because there are many more model parameters than experimental observables that can be used for fitting.

Applying metabolic control analysis to the kinetic model, we calculated which steps had the greatest control on the futile cycling ratio J_9/J_{11}. It is worth noting that the futile cycling control coefficients for all the steps sum to zero; this follows from the fact that $C_i^{J_9/J_{11}} = C_i^{J_9} - C_i^{J_{11}}$, and that the J_9- and J_{11}-control coefficients individually sum to unity (the summation theorem for flux-control coefficients [24,25]). Hence, some steps will lead to an increase in futile cycling, whereas others will decrease the J_9/J_{11} ratio (Figure 2). When the activities of all steps are increased by the same fractional amount, all the fluxes will increase by the same fractional amount and the metabolite concentrations will be unchanged; as a consequence the futile cycling ratio J_9/J_{11} will also be unchanged.

The activities of those steps with the numerically largest $C^{J_9/J_{11}}$ values were then varied 5-fold to analyse systematically the effects on futile cycling, the flux of sucrose accumulation, and the conversion efficiency from hexoses into sucrose. This allowed us to develop rational enhancement strategies: in view of the modelling results, overexpression of the fructose or glucose transporter or vacuolar sucrose importer, and reduction of invertase are the most promising targets (Figure 3). It should be noted that although decreasing hexokinase(Glc) levels reduced futile cycling, the flux of sucrose accumulation was decreased at the same time, which discounts this manipulation as a useful experimental enhancement strategy.

The construction of the kinetic model involved a number of simplifications. First, the vacuolar compartment was not modelled explicitly. The reasons for this were 3-fold: (i) at present, it is impossible to distinguish experimentally between cytosolic and vacuolar metabolite pools; (ii) there is insufficient information on the transport steps for sucrose, glucose and fructose across the vacuolar membrane; and (iii) the model presented here is a first approach at describing sucrose metabolism in sugar cane quantitatively, and in that should minimize the number of unknowns. Nevertheless, future extensions of this model should certainly include the vacuolar compartment, as it fulfils an important storage function. However, such an extension will preclude a steady-state analysis as presented in the present paper, since sucrose is continually accumulated in the vacuole during the sugar cane tissue maturation process and a true steady state is never established for the complete sucrose metabolism (including the vacuole). The results presented, therefore, at best approximate the quasi steady state in the cytosol for medium-mature sugar cane culm tissue (internode 5). However, it would be an interesting extension of this work to simulate the time-dependence of sucrose accumulation in sugar cane culm during the entire maturation process (i.e. extending over a period of months). This would require time-course kinetic modelling; in addition, one would need to know how the maximal activities of the enzymes change with time during the maturation process.

A second simplification entailed the clamping of the concentrations of the metabolic cofactors ATP, ADP, UDP and P_i at experimentally determined levels. In the living cell, these concentrations are free to vary. The reason for clamping them was that these cofactors participate in many more enzyme reactions than those explicated in the model, and their steady-state concentrations will be a function of all the reactions they participate in. We reasoned that fixing their concentrations at experimentally determined levels would give a more realistic representation of the system than calculating their concentration in the model on the basis of a clearly insufficient subset of reactions in which they participate. In a much larger model encompassing most of the reactions of central metabolism in sugar cane, the concentrations of the metabolic cofactors should of course be set free to vary. However, such a model is not yet available; indeed, the model reported here can serve as a basis for further extension to include the other pathways.

Apart from addressing the simplifying assumptions described above, other model extensions could include the simulation of metabolism in different internodes, to assess effects of tissue maturation on flux and concentration distributions. The model can also be used to simulate metabolic behaviour in other plant tissues (e.g. leaves or roots) if the appropriate enzyme activity levels are known. The other kinetic parameters can be used unchanged, unless tissue-specific isoenzymes are expressed. This would prove a valuable extension of the present model, because carbohydrate flux distributions and partitioning differ markedly between source and sink tissues.

We have used the kinetic model in the present paper to investigate rational enhancement strategies for improvement of sucrose accumulation in sugar cane (Figure 3). On the basis of these simulations, experiments are currently underway in our laboratory to decrease neutral invertase activity using antisense technology in transgenic sugar cane plants. Should the model predictions (Figure 3d) be borne out by these experimental results, this will provide additional validation for the model and give impetus to further *in silico* investigation of other possible manipulations towards sugar cane improvement.

In conclusion, the work in the present paper represents an example of an integrative approach to the analysis of the control and regulation of cellular systems [28]. The combination of quantitative experimentation with theoretical analysis and numerical simulation on the computer allows us to develop strategies for rationally manipulating these systems to our own advantage. More importantly, however, a kinetic model increases our understanding of such complex systems and enables us to describe their behaviour and regulation in a quantitative way.

J.M.R. thanks his fellow members of the Triple-J Group for Molecular Cell Physiology (Jannie Hofmeyr and Jacky Snoep) for helpful discussions. Jacky Snoep and Brett Olivier (Department of Biochemistry, University of Stellenbosch) helped with the WWW-based model implementation in Java and Mathematica. This work was supported by the South African National Research Foundation and the South African Sugar Association.

APPENDIX

Rate equations used in the model

Literature references for kinetic details and parameter values are given in Table 1.

Fructose uptake and glucose uptake

Fructose uptake (Figure 1, reaction 1) and glucose uptake (reaction 2) were modelled with irreversible Michaelis–Menten kinetics, with the intracellular sugar acting as a competitive inhibitor of the respective transport system:

$$v_1 = V_{\max 1}\frac{[\mathrm{Fru_{ex}}]}{K_{\mathrm{m\ Fru_{ex}}}(1+[\mathrm{Fru}]/K_{\mathrm{i\ Fru}})+[\mathrm{Fru_{ex}}]} \tag{A1}$$

$$v_2 = V_{\max 2}\frac{[\mathrm{Glc_{ex}}]}{K_{\mathrm{m\ Glc_{ex}}}(1+[\mathrm{Glc}]/K_{\mathrm{i\ Glc}})+[\mathrm{Glc_{ex}}]} \tag{A2}$$

Fru, fructose; Glc, glucose; subscript 'ex', extracellular concentration.

Hexokinase

Hexokinase activity was simulated using an irreversible random order bi-reactant mechanism. Because the enzyme can phosphorylate both glucose and fructose, the two phosphorylating activities were modelled in separate reactions (Figure 1, reaction 3 for glucose phosphorylation and reaction 4 for fructose phosphorylation). We included competitive inhibition of the activity by the sugar phosphate products, as well as competitive inhibition by the sugar substrate for the other activity (fructose for reaction 3 and glucose for reaction 4):

$$v_3 = V_{\max 3}\frac{\dfrac{[\mathrm{Glc}]}{K_{\mathrm{m\ Glc}}}\dfrac{[\mathrm{ATP}]}{K_{\mathrm{m\ ATP}}}}{\left(1+\dfrac{[\mathrm{ATP}]}{K_{\mathrm{m\ ATP}}}\right)\left(1+\dfrac{[\mathrm{Glc}]}{K_{\mathrm{m\ Glc}}}+\dfrac{[\mathrm{Fru}]}{K_{\mathrm{m\ Fru}}}+\dfrac{[\mathrm{Glc6P}]}{K_{\mathrm{i\ Glc6P}}}+\dfrac{[\mathrm{Fru6P}]}{K_{\mathrm{i\ Fru6P}}}\right)} \tag{A3}$$

$$v_4 = V_{\max 4}\frac{\dfrac{[\mathrm{Fru}]}{K_{\mathrm{m\ Fru}}}\dfrac{[\mathrm{ATP}]}{K_{\mathrm{m\ ATP}}}}{\left(1+\dfrac{[\mathrm{ATP}]}{K_{\mathrm{m\ ATP}}}\right)\left(1+\dfrac{[\mathrm{Glc}]}{K_{\mathrm{m\ Glc}}}+\dfrac{[\mathrm{Fru}]}{K_{\mathrm{m\ Fru}}}+\dfrac{[\mathrm{Glc6P}]}{K_{\mathrm{i\ Glc6P}}}+\dfrac{[\mathrm{Fru6P}]}{K_{\mathrm{i\ Fru6P}}}\right)} \tag{A4}$$

Fructokinase

There exists a separate fructokinase enzyme in sugar cane, which is only able to phosphorylate fructose and not glucose. This enzyme was modelled with irreversible random order bi-reactant kinetics, including competitive inhibition by ADP and non-competitive inhibition by the substrate fructose:

$$v_5 = \frac{V_{\max 5}}{1+\dfrac{[\mathrm{Fru}]}{K_{\mathrm{i\ Fru}}}}\times\frac{\dfrac{[\mathrm{Fru}]}{K_{\mathrm{m\ Fru}}}\dfrac{[\mathrm{ATP}]}{K_{\mathrm{m\ ATP}}}}{1+\dfrac{[\mathrm{Fru}]}{K_{\mathrm{m\ Fru}}}+\dfrac{[\mathrm{ATP}]}{K_{\mathrm{m\ ATP}}}+\dfrac{[\mathrm{Fru}]\,[\mathrm{ATP}]}{K_{\mathrm{m\ Fru}}K_{\mathrm{m\ ATP}}}+\dfrac{[\mathrm{ADP}]}{K_{\mathrm{i\ ADP}}}} \tag{A5}$$

Sucrose phosphate synthase

Sucrose phosphate synthase (Figure 1, reaction 6) activity was modelled with a reversible ordered bi-reactant mechanism, with UDP-glucose binding first and UDP dissociating last from the enzyme. The enzyme activity was defined positive in the direction of sucrose phosphate synthesis. P_i was a competitive inhibitor with respect to fructose 6-phosphate:

$$v_6 = V_{\mathrm{f6}}\frac{[\mathrm{Fru6P}][\mathrm{UDPGlc}]-\dfrac{[\mathrm{Suc6P}][\mathrm{UDP}]}{K_{\mathrm{eq6}}}}{[\mathrm{Fru6P}][\mathrm{UDPGlc}]\left(1+\dfrac{[\mathrm{Suc6P}]}{K_{\mathrm{i\ Suc6P}}}\right)+K_{\mathrm{m\ Fru6P}}\left(1+\dfrac{[P_i]}{K_{\mathrm{i}\,P_i}}\right)([\mathrm{UDPGlc}]+K_{\mathrm{i\ UDPGlc}})+K_{\mathrm{m\ UDPGlc}}[\mathrm{Fru6P}]+\dfrac{V_{\mathrm{f6}}}{V_{\mathrm{r6}}K_{\mathrm{eq6}}}}$$
$$\times\left[[\mathrm{Suc6P}]K_{\mathrm{m\ UDP}}\left(1+\frac{[\mathrm{UDPGlc}]}{K_{\mathrm{i\ UDPGlc}}}\right)+[\mathrm{UDP}]\left\{K_{\mathrm{m\ Suc6P}}\left(1+\frac{K_{\mathrm{m\ UDPGlc}}[\mathrm{Fru6P}]}{K_{\mathrm{i\ UDPGlc}}K_{\mathrm{m\ Fru6P}}(1+[P_i]/K_{\mathrm{i}P_i})}\right)+[\mathrm{Suc6P}]\left(1+\frac{[\mathrm{Fru6P}]}{K_{\mathrm{i\ Fru6P}}}\right)\right\}\right] \tag{A6}$$

Sucrose phosphatase

Sucrose phosphatase (Figure 1, reaction 7) activity was modelled as an irreversible Michaelis–Menten mechanism:

$$v_7 = V_{\max 7}\frac{[\text{Suc6P}]}{K_{\text{m Suc6P}} + [\text{Suc6P}]} \tag{A7}$$

Sucrose synthase

Sucrose synthase (Figure 1, reaction 8) activity was modelled with a reversible ordered bi-reactant mechanism, with UDP-glucose binding first and UDP dissociating last from the enzyme:

$$v_8 = -V_{\text{f8}}\frac{[\text{Suc}][\text{UDP}] - \dfrac{[\text{Fru}][\text{UDPGlc}]}{K_{\text{eq8}}}}{[\text{Suc}][\text{UDP}]\left(1+\dfrac{[\text{Fru}]}{K_{\text{i Fru}}}\right) + K_{\text{m Suc}}([\text{UDP}]+K_{\text{i UDP}}) + K_{\text{m UDP}}[\text{Suc}] + \dfrac{V_{\text{f8}}}{V_{\text{r8}}K_{\text{eq8}}}\left[[\text{Fru}]K_{\text{m UDPGlc}}\left(1+\dfrac{[\text{UDP}]}{K_{\text{i UDP}}}\right)\right.}$$
$$\left. + [\text{UDPGlc}]\left\{K_{\text{m Fru}}\left(1+\frac{K_{\text{m UDP}}[\text{Suc}]}{K_{\text{i UDP}}K_{\text{m Suc}}}\right) + [\text{Fru}]\left(1+\frac{[\text{Suc}]}{K_{\text{i Suc}}}\right)\right\}\right] \tag{A8}$$

The maximal activities and equilibrium constant in eqn (A8) are defined for the reaction proceeding in the direction of fructose synthesis, as the enzyme is most commonly assayed in this direction. However, the model calculated the flux through reaction 8 to proceed in the direction of sucrose synthesis; hence, we defined this direction as positive and preceded the rate equation with a minus sign.

Neutral invertase

Neutral (cytosolic) invertase (Figure 1, reaction 9) activity was modelled as an irreversible Michaelis–Menten mechanism with competitive inhibition by fructose and non-competitive inhibition by glucose. As the mechanism of inhibition has not been determined in sugar cane, we assumed it to be the same as for carrot neutral invertase [29]:

$$v_9 = \frac{V_{\max 9}}{1+[\text{Glc}]/K_{\text{i Glc}}} \times \frac{[\text{Suc}]}{K_{\text{m Suc}}(1+[\text{Fru}]/K_{\text{i Fru}})+[\text{Suc}]} \tag{A9}$$

Lower glycolysis

The lower part of glycolysis (Figure 1, reaction 10) was modelled as a single reaction proceeding from fructose 6-phosphate, following irreversible Michaelis–Menten kinetics:

$$v_{10} = V_{\max 10}\frac{[\text{Fru6P}]}{K_{\text{m Fru6P}} + [\text{Fru6P}]} \tag{A10}$$

Vacuolar sucrose accumulation

Sucrose accumulation into the vacuole (Figure 1, reaction 11) was modelled as a reaction proceeding from cytosolic sucrose, following irreversible Michaelis–Menten kinetics:

$$v_{11} = V_{\max 11}\frac{[\text{Suc}]}{K_{\text{m Suc}} + [\text{Suc}]} \tag{A11}$$

UDP-glucose pyrophosphorylase, phosphoglucomutase and phosphoglucoisomerase

The enzymes UDP-glucose pyrophosphorylase, phosphoglucomutase and phosphoglucoisomerase were modelled as a single block, with the reactions assumed to be in equilibrium. This assumption was justified by experimentally determined mass-action ratios being close to the equilibrium constant under a variety of conditions [30,31]. The reactions 3–6, 8 and 10 were thus simulated as interconverting a single hexose phosphate pool, and the concentrations of UDP-glucose, glucose 1-phosphate, glucose 6-phosphate and fructose 6-phosphate were calculated by distributing the hexose phosphate pool according to the equilibrium constants of the three reactions (see also Table 1).

Differential equations

The steady-state behaviour of the kinetic model was simulated by simultaneously solving the following set of differential equations and setting them equal to zero:

$$\text{d}[\text{Glc}]/\text{d}t = v_2 - v_3 + v_9 \tag{A12}$$

$$d[Fru]/dt = v_1 - v_4 - v_5 - v_8 + v_9 \quad (A13)$$

$$d[HexP]/dt = v_3 + v_4 + v_5 - 2v_6 - v_8 - v_{10} \quad (A14)$$

$$d[Suc6P]/dt = v_6 - v_7 \quad (A15)$$

$$d[Suc]/dt = v_7 + v_8 - v_9 - v_{11} \quad (A16)$$

REFERENCES

1 Moore, P. H. (1995) Temporal and spatial regulation of sucrose accumulation in the sugarcane. Aust. J. Plant Physiol. **22**, 661–679
2 Moore, P. H. and Maretzki, A. (1996) Sugarcane. In Photoassimilate Distribution in Plants and Crops: Source-Sink Relationships (Zamski, E. and Schaffer, A. A., eds.), pp. 643–669, Marcel Dekker Inc., New York
3 Whittaker, A. and Botha, F. C. (1997) Carbon partitioning during sucrose accumulation in sugarcane internodal tissue. Plant Physiol. **115**, 1651–1659
4 Botha, F. C. and Black, K. G. (2000) Sucrose phosphate synthase and sucrose synthase activity during maturation of internodal tissue in sugarcane. Aust. J. Plant Physiol. **27**, 81–85
5 Stitt, M. and Sonnewald, U. (1995) Regulation of metabolism in transgenic plants. Annu. Rev. Plant Physiol. Plant Mol. Biol. **46**, 341–368
6 Batta, S. K. and Singh, R. (1986) Sucrose metabolism in sugar cane grown under varying climatic conditions: Synthesis and storage of sucrose in relation to the activities of sucrose synthase, sucrose-phosphate synthase and invertase. Phytochemistry **25**, 2431–2437
7 Sacher, J. A., Hatch, M. D. and Glasziou, K. T. (1963) Sugar accumulation cycle in sugar cane. III. Physical and metabolic aspects of cycle in immature storage tissues. Plant Physiol. **38**, 348–354
8 Wendler, R., Veith, R., Dancer, J., Stitt, M. and Komor, E. (1990) Sucrose storage in cell suspension cultures of *Saccharum* sp. (sugarcane) is regulated by a cycle of synthesis and degradation. Planta **183**, 31–39
9 Hatch, M. D. and Glasziou, K. T. (1963) Sugar accumulation cycle in sugar cane. II. Relationship of invertase activity to sugar content and growth rate storage tissue of plants grown in controlled environments. Plant Physiol. **38**, 344–348
10 Gayler, K. R. and Glasziou, K. T. (1972) Sugar accumulation in sugarcane. Plant Physiol. **49**, 563–568
11 Zhu, Y. J., Komor, E. and Moore, P. H. (1997) Sucrose accumulation in the sugarcane stem is regulated by the difference between the activities of soluble acid invertase and sucrose phosphate synthase. Plant Physiol. **115**, 609–616
12 Vorster, D. J. and Botha, F. C. (1999) Sugercane internodal invertases and tissue maturity. J. Plant Physiol. **155**, 470–476
13 Lingle, S. E. and Smith, R. C. (1991) Sucrose metabolism related to growth and ripening in sugarcane internodes. Crop Sci. **31**, 172–177
14 Schuster, S., Dandekar, T. and Fell, D. A. (1999) Detection of elementary flux modes in biochemical networks: a promising tool for pathway analysis and metabolic engineering. Trends Biotechnol. **17**, 53–60
15 Schuster, S., Fell, D. A. and Dandekar, T. (2000) A general definition of metabolic pathways useful for systematic organization and analysis of complex metabolic networks. Nat. Biotechnol. **18**, 326–332
16 Bakker, B. M., Michels, P. A. M., Opperdoes, F. R. and Westerhoff, H. V. (1997) Glycolysis in bloodstream form *Trypanosoma brucei* can be understood in terms of the kinetics of the glycolytic enzymes. J. Biol. Chem. **272**, 3207–3215
17 Rohwer, J. M., Meadow, N. D., Roseman, S., Westerhoff, H. V. and Postma, P. W. (2000) Understanding glucose transport by the bacterial phosphoenolpyruvate:glycose phosphotransferase system on the basis of kinetic measurements *in vitro*. J. Biol. Chem. **275**, 34909–34921
18 Schuster, S. and Hilgetag, C. (1994) On elementary flux modes in biochemical reaction systems at steady state. J. Biol. Syst. **2**, 165–182
19 Komor, E. (2000) The physiology of sucrose storage in sugarcane. In Carbohydrate Reserves in Plants – Synthesis and Regulation (Gupta, A. K. and Kaur, N., eds.), pp. 35–54, Elsevier Science, Amsterdam
20 Pfeiffer, T., Sánchez-Valdenebro, I., Nuño, J. C., Montero, F. and Schuster, S. (1999) METATOOL: for studying metabolic networks. Bioinformatics **15**, 251–257
21 Sauro, H. M. (1993) SCAMP: a general-purpose simulator and metabolic control analysis program. Comput. Appl. Biosci. **9**, 441–450
22 Mendes, P. (1997) Biochemistry by numbers: simulation of biochemical pathways with Gepasi 3. Trends Biochem. Sci. **22**, 361–363
23 Komor, E. (1994) Regulation by futile cycles: the transport of carbon and nitrogen in plants. In Flux Control in Biological Systems (Schulze, E. D., ed.), pp. 153–201, Academic Press, San Diego
24 Kacser, H. and Burns, J. A. (1973) The control of flux. Symp. Soc. Exp. Biol. **27**, 65–104
25 Heinrich, R. and Rapoport, T. A. (1974) A linear steady-state treatment of enzymatic chains. General properties, control and effector strength. Eur. J. Biochem. **42**, 89–95
26 Kholodenko, B. N., Molenaar, D., Schuster, S., Heinrich, R. and Westerhoff, H. V. (1995) Defining control coefficients in non-ideal metabolic pathways. Biophys. Chem. **56**, 215–226
27 Schuster, S. and Heinrich, R. (1992) The definitions of metabolic control analysis revisited. BioSystems **27**, 1–15
28 Rohwer, J. M. and Hofmeyr, J.-H. S. (2000) An integrated approach to the analysis of the control and regulation of cellular systems. In Technological and Medical Implications of Medical Control Analysis (Cornish-Bowden, A. and Cárdenas, M. L., eds.), pp. 73–79, Kluwer Academic Publishers, Dordrecht
29 Lee, H.-S. and Sturm, A. (1996) Purification and characterization of neutral and alkaline invertase from carrot. Plant Physiol. **112**, 1513–1522
30 Kruger, N. J. (1997) Carbohydrate synthesis and degradation. In Plant Metabolism (Dennis, D. T., Turpin, D. H., Lefebvre, D. D. and Layzell, D. B., eds.), pp. 83–104, Longman, Essex
31 Stitt, M. and Steup, M. (1985) Starch and sucrose degradation. In Higher Plant Cell Respiration (Douce, R. and Day, D. A., eds.), pp. 347–390, Springer-Verlag, Heidelberg
32 Bindon, K. A. (2000) Carbon partitioning in sugarcane internodal tissue with special reference to the insoluble fraction. Master's thesis, University of Stellenbosch
33 Komor, E., Thom, M. and Maretzki, A. (1981) The mechanism of sugar uptake by sugarcane suspension cells. Planta **153**, 181–192
34 Botha, F. C., Whittaker, A., Vorster, D. J. and Black, K. G. (1996) Sucrose accumulation rate, carbon partitioning and expression of key enzyme activities in sugarcane stem tissue. In Sugarcane: Research Towards Efficient and Sustainable Production (Wilson, J. R., Hogarth, D. M., Campbell, J. A. and Garside, A. L., eds.), pp. 98–101, CSIRO division of Tropical Crops and Pastures, Brisbane
35 Whittaker, A. (1997) Pyrophosphate dependent phosphofructokinase (PFP) activity and other aspects of sucrose metabolism in sugarcane internodal tissues. Ph.D. thesis, University of Natal
36 Pego, J. V. and Smeekens, S. C. M. (2000) Plant fructokinases: a sweet family get-together. Trends Plant Sci. **5**, 531–536
37 Renz, A. and Stitt, M. (1993) Substrate specificity and product inhibition of different forms of fructokinases and hexokinases in developing potato tubers. Planta **190**, 166–175
38 Doehlert, D. C. (1989) Separation and characterization of four hexose kinases from developing maize kernels. Plant Physiol. **89**, 1042–1048
39 Chaubron, F., Harris, N., Ross, H. A. and Davies, H. V. (1995) Partial purification and characterization of fructokinase from developing taproots of sugar beet (*Beta vulgaris*). Plant Sci. **110**, 181–186
40 Huber, S. C. and Huber, J. L. (1996) Role and regulation of sucrose-phosphate synthase in higher plants. Annu. Rev. Plant Physiol. Mol. Biol. **47**, 431–444
41 Quick, W. P. and Schaffer, A. A. (1996) Sucrose metabolism in sources and sinks. In Photoassimilate Distribution in Plants and Crops: Source-Sink Relationships (Zamski, E. and Schaffer, A. A., eds.), pp. 115–156, Marcel Dekker Inc., New York
42 Buczynski, S. R., Thom, M., Chourey, P. and Maretzki, A. (1993) Tissue distribution and characterization of sucrose synthase isozymes in sugarcane. J. Plant Physiol. **142**, 641–646
43 Vorster, D. J. and Botha, F. C. (1998) Partial purification and characterisation of sugarcane neutral invertase. Phytochem. **49**, 651–655
44 Bindon, K. and Botha, F. C. (2000) Tissue disks as an experimental system for metabolic flux analysis in the sugarcane culm. South Afr. J. Bot. **66**, 260–264
45 Dancer, J., Veith, R., Feil, R., Komor, E. and Stitt, M. (1990) Independent changes of inorganic pyrophosphate and the ATP/ADP or UTP/UDP ratios in plant cell suspension cultures. Plant Sci. **66**, 59–63

Received 19 March 2001/24 May 2001; accepted 20 June 2001